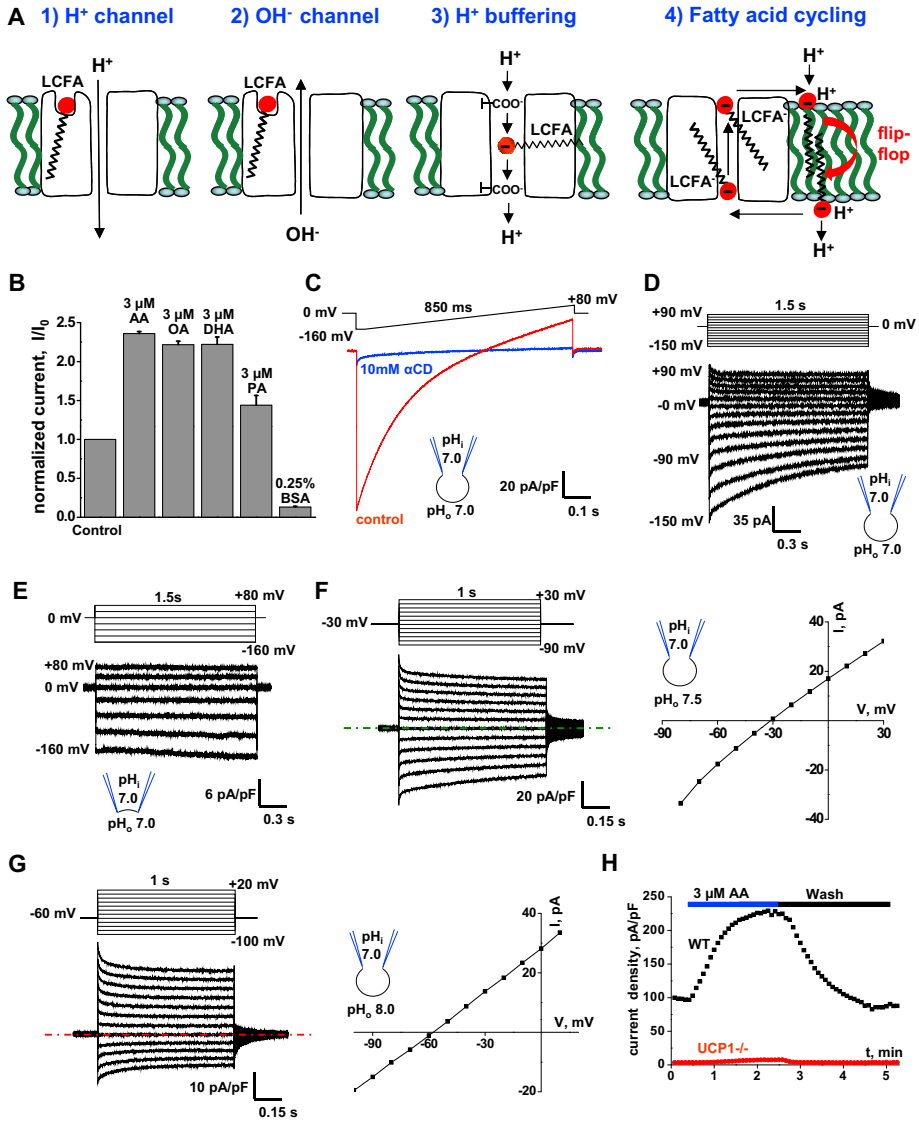

Figure S1. Electrophysiological Properties of UCP1 Current, Related to Figure 1

(A) Proposed models of UCP1 operation (from left to right): (1) H^+ channel activated by allosteric binding of LCFAs; (2) OH^- channel activated by allosteric binding of LCFAs; (3) the H^+ buffering model; (4) the fatty-acid cycling model.

(B) Mean normalized amplitudes of the whole-mitoplast putative UCP1 current measured before (control) and after addition of 3 μM arachidonic acid (AA), oleic acid (OA), docosahexaenoic acid (DHA), palmitoleic acid (PA), or 0.25% BSA to the bath solution; n = 4–18. Current amplitudes were measured upon stepping from 0 to −160 mV (see voltage protocol in Figure 1C) and normalized to the control value. The leak current was not subtracted.

(C) The whole-mitoplast putative UCP1 current (control, red) is inhibited by 10 mM αCD (blue). The voltage protocol is indicated at the top. The pipette-mitoplast diagram indicates the recording conditions.

(D) The whole-mitoplast I_{UCP1} in response to voltage steps from a holding potential of 0 mV; ΔV = 20 mV.

(E) Inside-out I_{UCP1} in response to voltage steps from a holding potential of 0 mV, ΔV = 40 mV. The BSA-insensitive leak current was subtracted.

(F) Left panel: Whole-mitoplast I_{UCP1} recorded at ΔpH = 0.5 in response to the voltage step protocol indicated at the top of the panel; ΔV = 10 mV. A holding potential of −30 mV (close to the E_H) was selected to minimize I_{UCP1} between applications of voltage steps and to eliminate depletion of the proton buffer inside the mitoplast (see Experimental Procedures). A zero current level is indicated by the green dotted line. Right panel: The I/V curve corresponding to the current traces in the left panel. Note the reversal potential. The pH values in the pipette and bath solutions are as indicated on the diagram.

(G) Left panel: Whole-mitoplast I_{UCP1} recorded at ΔpH = 1 in response to the voltage step protocol indicated at the top of the panel; ΔV = 20 mV. A holding potential of −60 mV (close to E_H) was selected to minimize depletion of proton buffer inside the mitoplast between voltage steps. A zero current level is indicated by the red dotted line. Right panel: The I/V curve corresponding to the current traces in the left panel. Note the reversal potential. The pH values in the pipette and bath solutions are as indicated on the diagram.

(H) Representative time-course activation of the whole-mitoplast current by 3 μM AA in wild-type (WT, black) and UCP1$^{-/-}$ (red) mice. Current amplitudes were measured upon stepping from 0 to −160 mV as in Figure 1C.

Error bars represent SEM.

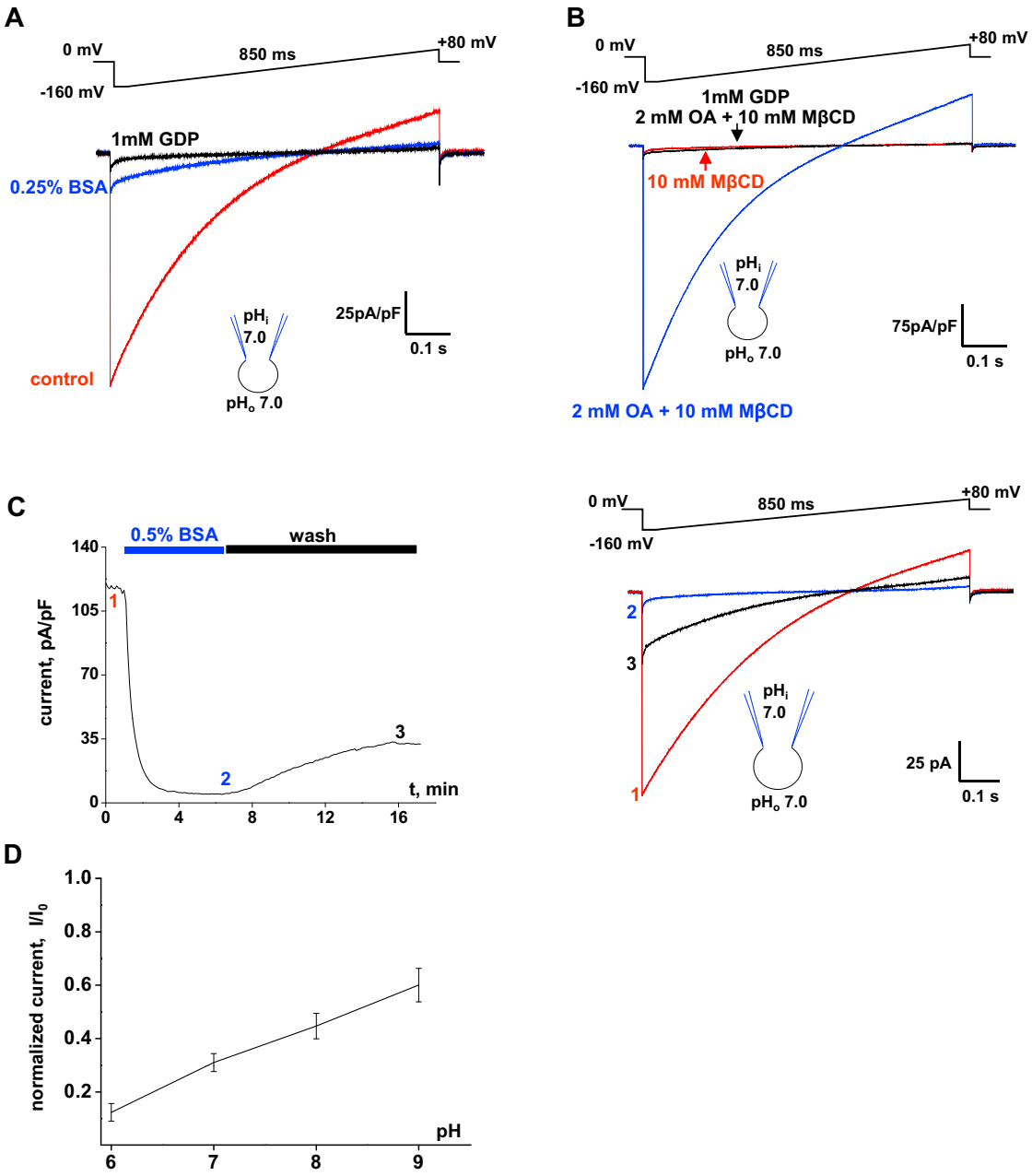

Figure S2. UCP1 Is Activated by LCFAs, Related to Figure 2

(A) Representative I_{UCP1} in control (red), upon extraction of endogenous LCFAs with 0.25% BSA (blue), and in 1 mM GDP (black).

(B) Representative I_{UCP1} upon extraction of endogenous LCFAs with 10 mM MβCD (red), after application of 2 mM OA mixed with 10 mM MβCD (blue), and upon application of 2 mM OA/10 mM MβCD with 1 mM GDP (black).

(C) Left panel: Representative time course of I_{UCP1} amplitude in control (1) and after the application (2) and subsequent washout (3) of 0.5% BSA at pH 7.0. I_{UCP1} amplitudes were measured upon stepping from 0 to −160 mV (see right panel). Right panel: I_{UCP1} traces recorded at times 1, 2, and 3 as indicated in the left panel.

(D) Graph showing the fraction of I_{UCP1} recovered after deactivation with 10 mM αCD at different symmetrical pH values.

Error bars represent SEM.

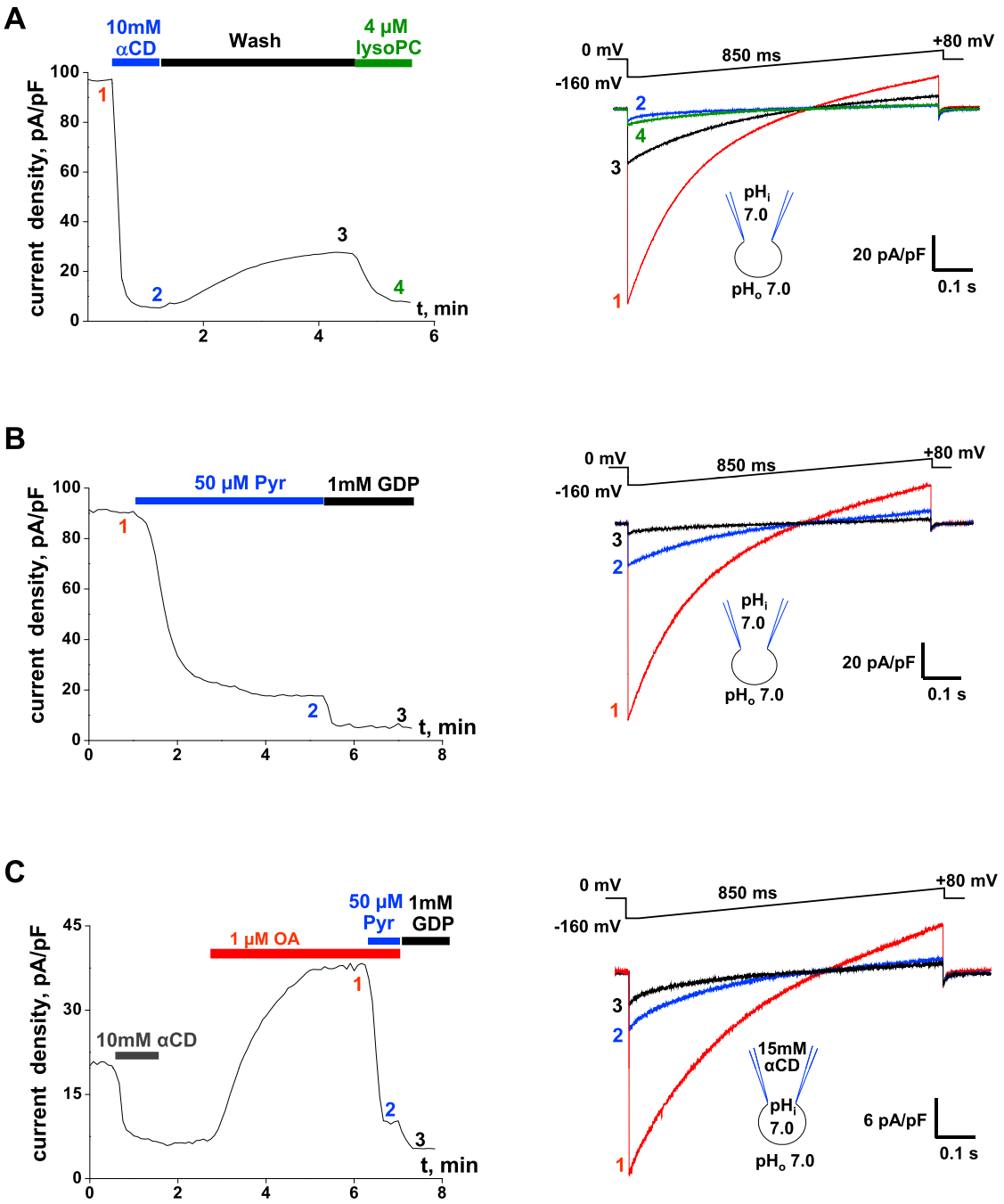

Figure S3. Regulation of I_{UCP1} by PLA2 Inhibitors, Related to Figure 3

(A) Left panel: Representative time course of the I_{UCP1} amplitude in control (1), after the extraction of endogenous LCFAs with 10 mM αCD (2), after the reactivation of I_{UCP1} by endogenous membrane LCFAs upon washout of αCD (3), and upon subsequent application of 4 μM oleoyl-lysoPC (4). I_{UCP1} amplitudes were measured upon stepping from 0 to −160 mV (see right panel). Right panel: I_{UCP1} traces recorded at times 1, 2, 3, and 4 as indicated in the left panel.

(B) Left panel: Representative time course of I_{UCP1} amplitude in control (1), upon the application of 50 μM pyrrophenone (Pyr, 2), and with the subsequent application 1 mM GDP (3). I_{UCP1} amplitudes were measured upon stepping from 0 to −160 mV (see right panel). Right panel: I_{UCP1} traces recorded at times 1, 2, and 3 as indicated in the left panel.

(C) Left panel: Representative time course of the I_{UCP1} amplitude after the extraction of endogenous LCFAs with 10 mM αCD, the reactivation of I_{UCP1} with 1 μM of OA (1), the subsequent addition of 50 μM pyrrophenone (2), and the application of 1 mM GDP (3). The pipette solution contained 15 mM αCD to extract endogenous LCFAs. I_{UCP1} amplitudes were measured upon stepping from 0 to −160 mV (see right panel). Right panel: I_{UCP1} traces recorded at times 1, 2, and 3 as indicated in the left panel.

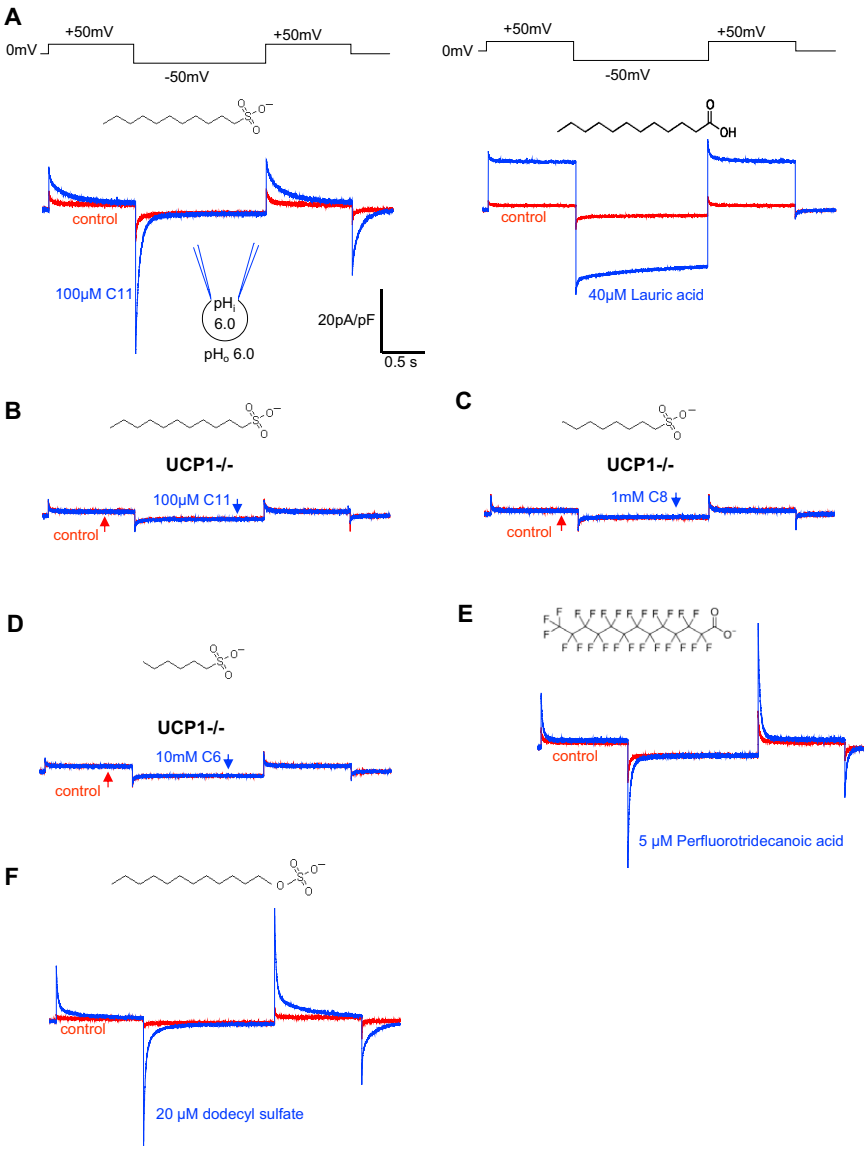

Figure S4. Currents Caused by Low-pKa LCFA Analogs in Wild-Type and UCP1$^{-/-}$ Mitoplasts, Related to Figure 4

(A) Left panel: Representative whole-mitoplast I_{UCP1} recorded upon extraction of endogenous membrane LCFAs with αCD (control, red) and after subsequent activation with 100 μM C11-sulfonate (blue). The experiment was performed at symmetrical pH 6.0. These traces are also shown in Figure 4B, left panel. Voltage protocol and structure of C11-sulfonate are shown at the top of the panel. The pipette-mitoplast diagram indicates the recording conditions. Right panel: I_{UCP1} activated by 40 μM lauric acid (C11-carboxylate) under the same recording conditions as in the left panel.

(B–D) Currents induced by 100 μM C11-sulfonate, 1 mM C8-sulfonate, and 10 mM C6-sulfonate, respectively, in UCP1$^{-/-}$ mitoplasts. See (A) for recording conditions and calibration bars.

(E and F) I_{UCP1} induced by 5 μM perfluorotridecanoic acid and 20 μM dodecyl sulfate, respectively, in wild-type mitoplasts. See (A) for recording conditions and calibration bars.

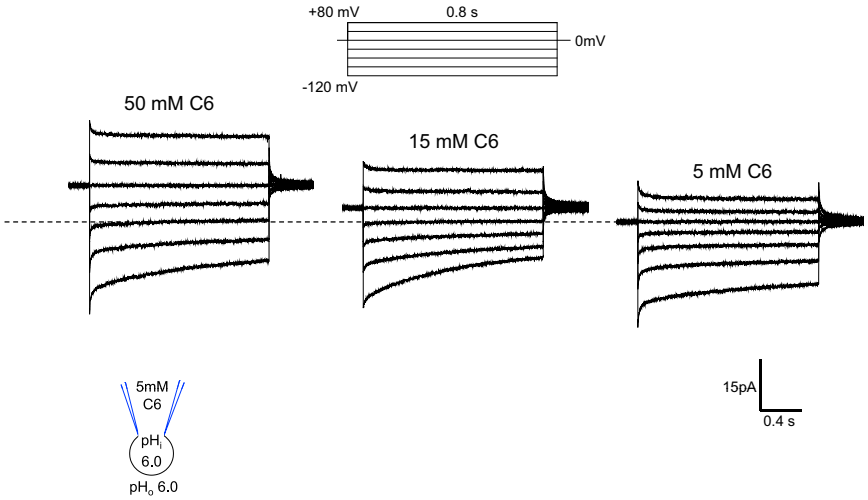

Figure S5. I_{UCP1} at Different Transmembrane Gradients of C6-Sulfonate, Related to Figure 5

I_{UCP1} carried by C6-sulfonate at pH 6.0 in the presence of 5 mM C6-sulfonate in the pipette and varying concentrations of C6-sulfonate (50 mM, 15 mM, and 5 mM) in the bath solution. The voltage protocol is shown at the top, and the pipette-mitoplast diagram indicates the recording conditions. The zero current level is indicated by the dotted line.

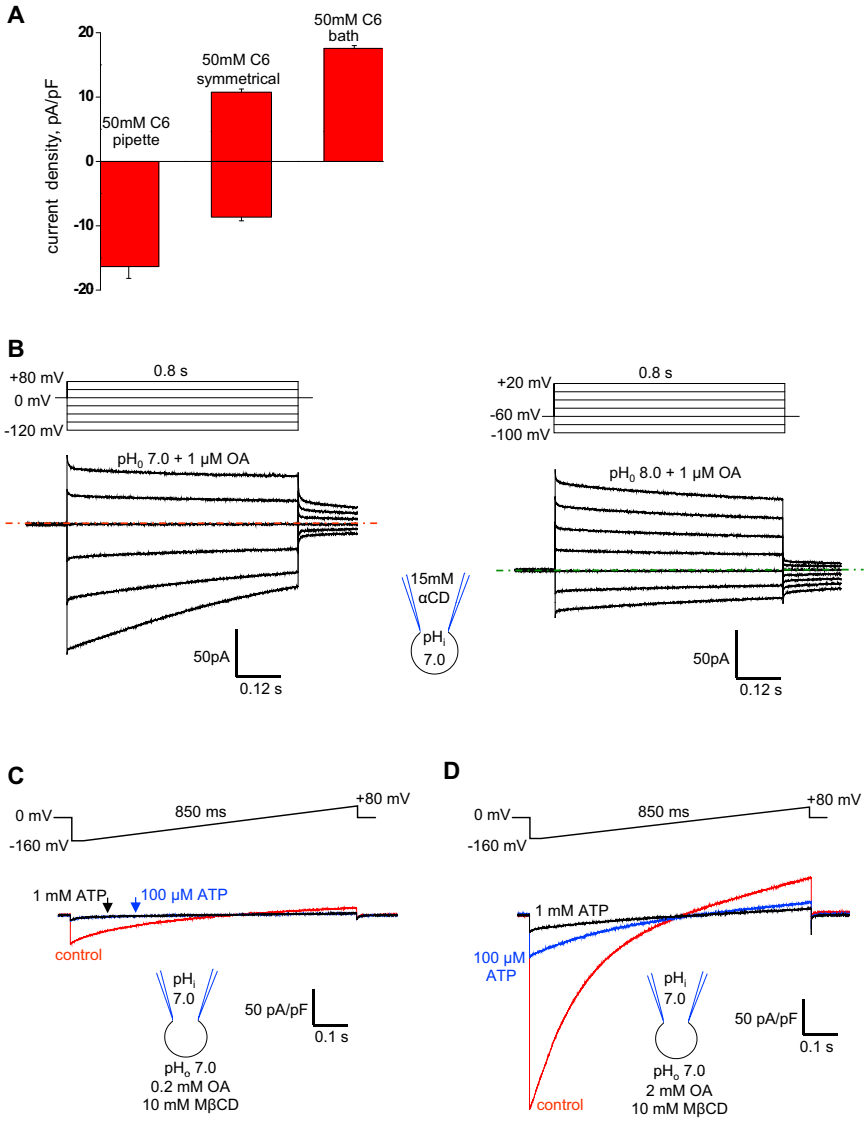

Figure S6. Asymmetry of Substrate Binding to UCP1, Related to Figure 6

(A) The mean amplitude of I_{UCP1} carried by C6-sulfonate, recorded with either 50 mM C6-sulfonate in the pipette, 50 mM C6-sulfonate in the bath, or symmetrical 50 mM C6-sulfonate, n = 4. I_{UCP1} was measured in the beginning of the second (−50 mV, inward I_{UCP1}) and third (+50 mV, outward I_{UCP1}) voltage steps; see Figure 6D.

(B) Left panel: Representative I_{UCP1} recorded with 15 mM αCD in the pipette solution and 1 μM OA in the bath solution. Both bath and pipette solutions had pH values of 7.0. The voltage step protocol is indicated at the top of the panel; ΔV = 40 mV. Right panel: I_{UCP1} recorded from the same mitoplast after the pH in the bath solution was changed to 8.0. The holding potential was changed to −60 mV to eliminate depletion of the proton buffer inside the mitoplast between voltage steps. The zero current level is indicated by the dotted lines. The pipette-mitoplast diagram indicates the recording conditions. The I_{UCP1} amplitude measured at the beginning of the voltage steps was used to plot the UCP1 I/V curves in Figure 6E.

(C) Representative I_{UCP1} induced by 0.2 mM OA mixed with 10 mM MβCD in control (red), and in the presence of 100 μM (blue) and 1 mM (black) ATP. Note that the blue and the black traces coincide.

(D) Representative I_{UCP1} induced by 2 mM OA mixed with 10 mM MβCD in control (red), and in the presence of 100 μM (blue) and 1 mM (black) ATP.

Error bars represent SEM.

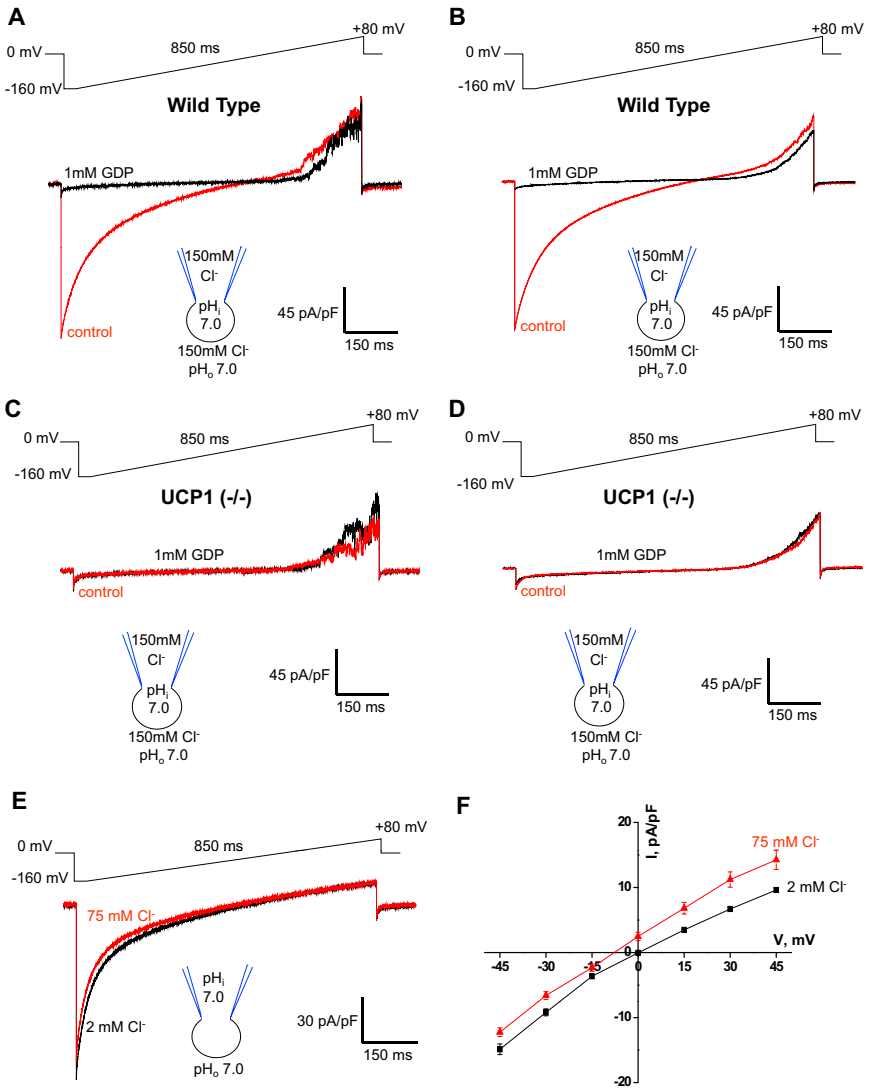

Figure S7. Cl^- Conductance of the IMM of BAT Is Primarily UCP1 Independent, Related to Figure 1

(A) Representative whole-mitoplast currents recorded from a wild-type mitoplast in symmetrical 150 mM Cl^- in control (red) and after the addition of 1 mM GDP (black).

(B) The same experiment as in (A), but each trace represents an average of 30–40 original current traces to smooth out fluctuations in the outward Cl^- current mediated by the large-conductance 108 pS anion channel (IMAC).

(C) Representative whole-mitoplast currents recorded from a UCP1$^{-/-}$ mitoplast in symmetrical 150 mM Cl^- in control (red) and after addition of 1 mM GDP (black).

(D) The same experiment as in (C), but each trace represents an average of 30–40 original current traces to smooth out fluctuations in the outward Cl^- current mediated by the large-conductance 108 pS anion channel (IMAC).

(E) Representative whole-mitoplast I_{UCP1} in a bath solution containing 2 mM (black) or 75 mM (red) Cl^-. Bath and pipette solutions contain 1 mM Mg^{2+} to inhibit the IMAC current. Note the absence of large-conductance IMAC openings at positive potentials even in the presence of 75 mM Cl^- in the bath (red trace).

(F) Current-voltage dependence of I_{UCP1} in a bath solution containing 2 mM (black) or 75 mM (red) Cl^- (n = 5). The I_{UCP1} was recorded at symmetrical pH 7.0. I_{UCP1} was measured with a voltage step protocol from the holding potential of 0 mV (not shown). Current amplitudes were measured at the beginning of voltage steps. Error bars represent SEM.